

## KINETICS AND EQUILIBRIUM ADSORPTION STUDIES OF REMOVAL OF ANIONIC DYES FROM WATER USING CALCINED LAYERED DOUBLE HYDROXIDES

P. B. SIBANDA<sup>1</sup>, S. MAJONI<sup>2</sup>, L. L. SIBALI<sup>3</sup> AND H. CHIRIRIWA<sup>4\*</sup>

<sup>1</sup>Department of Applied Chemistry, National University of Science and Technology, Bulawayo, Zimbabwe

<sup>2</sup>Department of Chemical & Forensic Sciences, Botswana International University of Science & Technology, Private Bag 16, Palapye, Botswana

<sup>3</sup>Department of Environmental Sciences, College of Agriculture and Environmental Sciences, University of South Africa, Florida, South Africa

<sup>4</sup>Department of Chemical Engineering, Vaal University of Technology, Private Bag X021, Vanderbijlpark, 1911, Andries Potgieter Blvd, South Africa

(Received 31 May, 2020; Accepted 27 July, 2020)

### ABSTRACT

Layered double hydroxides were synthesised by a co-precipitation method with Mg/ Al ratio 2:1. The precursor LDH was calcined to produce mixed metal oxides which were used to remove the Titan Yellow dye by adsorption. The adsorbent was studied as a function of contact time, initial dye concentration, and adsorbent dosage using experiments in batch mode. The equilibrium sorption were fitted into Langmuir, Freundlich, Tempkin, and Dubinin-Radushkevich isotherms. Of the four adsorption isotherms, the R<sup>2</sup> value of the Tempkin isotherm was the highest. The heat of sorption process established from Tempkin isotherm was 11.036 J/mol. Pseudo-first order, pseudo-second order kinetics and Elovich model parameters have been determined. The process of dye uptake follows second order kinetics with K<sub>2</sub>= 0.0242 mgg<sup>-1</sup>min<sup>-1</sup> and R<sup>2</sup>=0.9994. The results show that layered double hydroxides can be utilised as a substitute adsorbent to remove anionic dyes.

**KEY WORDS :** Layered Double Hydroxide, Intercalation, Calcination, Titan yellow, Adsorption

### INTRODUCTION

A variety of synthetic inorganic materials of well-defined structure and functionality materials possess useful properties which are useful in addressing today's environmental and industrial problems (Mir *et al.*, 2018). An estimated 10, 000 different dyes and pigments are used industrially and 0.7 million tons of synthetic dyes are produced across the globe and these dyes are released as effluents during the dyeing processes and more than 50% of these are azo dyes (Gomez *et al.*, 2007; Gupta *et al.*, 2013; Greluk and Hubicki, 2011, Marsch and Reinoso, 2006). Water pollution due to industrial activities like paper and pulp manufacturing, dyeing of cloth, textile, leather treatment, printing, food

production and other anthropogenic activities which use dyes, is a constantly growing problem (Zaharia and Suteu, 2012). Removal of anionic dyes is difficult as they are water soluble and they produce very bright colours in water with acidic properties. Dyes have aromatic molecular structures that are complex and are resistant to oxidizers, light and temperature (Banerjee and Chattopadhyaya, 2017). This property makes dyes non-degradable and thus bioaccumulate in living organisms, leading to disorders and severe diseases. Some of these dyes are toxic, carcinogenic causing skin and eye irritation (Sen and Dawood, 2014). Studies have shown that activated carbon is more effective than anionic dyes in removing cationic dyes (Pereira *et al.*, 2003; Al-Degs *et al.*, 2001).

Current methods regarding water treatment such as froth floating (Kyzas and Matis, 2018), ion exchange (Xu, 2005; Kurniawan *et al.*, 2006), coagulation (Shen *et al.*, 2011), ozonation (Mehrjouei *et al.*, 2015), nanofiltration (NF) (Kim *et al.*, 2007; Shon *et al.*, 2013) reverse osmosis (RO) (Perez *et al.*, 2010; Xu *et al.*, 2013) with polymeric membranes and chemical precipitation are increasingly used in the treatment and reuse of coloured waste water. However, the methods are not widely used due to high costs, less efficiency, limited applicability and they produce wastes, which are difficult to dispose of.

Layered double hydroxides (LDH) have special significance because their quality is similar to traditional intercalated substances, having nano-scale periodicity, achieving complete separation of charge between layers and gallery ions (Z̄umreoglu-Karan and Ay, 2012). The combination of Layered Double materials and intercalation techniques have allowed improved applications in many areas including biomaterials and in heterogeneous catalysis (Mishra *et al.*, 2018; Fan *et al.*, 2014). LDHs are novel because of their ease of preparation, inexpensiveness, and versatility (Sarfranz and Shakir, 2017). In addition they are also recyclable and have high anion exchange capacity. In the past decade, compelling headway has been achieved in the preparation of layered double hydroxides with new morphologies and compositions, which can be better applied to the removal of anionic dyes from effluent water. In this work, the adsorption properties of calcined Layered Double Hydroxides (cLDH) synthesized from aluminium nitrate and magnesium nitrate are investigated for the removal of Titan Yellow an anionic dye.

### Experimental Section

The investigation was carried out in batch experiments. All other factors were kept constant while the factor in question was varied. Every factor in question was run thrice for each set of constant factors and all experiments were carried out at room temperature.

### Chemicals

Titan yellow ( $C_{28}H_{19}N_5Na_2O_6S_4$ ) and all reagent grade chemicals were purchased from Sigma Aldrich and Merck Chemicals and used without further purification.

### Instrumentation

Elemental analysis was determined by XRF analysis on a Philips PW 2400 X-Ray Spectrometer. Fourier transform infrared spectroscopy (Thermoscientific Nicket IS10) was used to characterize the layered double hydroxides (LDH). PXRD analysis was performed using Bruker XRD with Ni-filtered Cu- $\alpha$  radiation ( $\lambda=1.54$  Å) at 40 KV and 30 mA. UV-Vis Spectrophotometer (Perkin Elmer Lambda 2) was used to determine the residual concentration of Titan Yellow in solution at maximum absorption wavelength,  $\lambda_{max}=410$  nm.

### LDH Preparation

#### Co-precipitation

The magnesium aluminium-carbonate LDH was synthesised by a co-precipitation method in a molar ratio (Mg/Al) of 2:1. Mixed metal nitrate solution was prepared by dissolving 128.21 g  $Mg(NO_3)_2 \cdot 6H_2O$  and 93.78 g of  $Al(NO_3)_3 \cdot 9H_2O$  in 1000 mL distilled water. The caustic solution was prepared by slowly dissolving 80.02 g of NaOH and 16.91 g  $Na_2CO_3$  in 1000 mL distilled water. The mixed metal solution was added dropwise from a separation funnel to the caustic solution while stirring. The pH was monitored using a pH probe and maintained at 10 by adding sodium hydroxide solution. A white precipitate of hydrotalcite was collected by vacuum filtration, washed several times with 0.1 M  $Na_2CO_3$  solution and dried in an oven at 80 °C for 48 hours.

#### Calcination and reformation

The hydrotalcite was calcined at 450 °C for 3 hours to form mixed metal oxides. The calcined layered double hydroxide was left to stand in the dye solution for 48 hours. The mixture was separated by vacuum filtration. The solid recovered was dried in an oven at 80 °C for 48 hours.

#### Effect of Titan Yellow concentration

Use 20-100 ppm Titan Yellow concentration range for batch adsorption experiments. Add 50 mL of Titan Yellow solution to a beaker containing 0.8 g of layered double oxide (LDO). Equilibrium time determined was used for each stirring experiment.

#### Effect of Layered Double Oxide dosage

This can be done by changing the LDO dose in the range of 0.2-1.0 g (increasing 0.2 g per run). A 50 mL volume of 20 ppm Titan Yellow solution was added

to the beaker containing the weighed LDO, and the mixture was stirred. All other parameters are fixed under the optimal conditions determined by experiments.

### Percentage Titan Yellow uptake and adsorption capacity

The amount of Titan Yellow adsorbed by calcined layered double hydroxide was calculated by applying equations (1) and (2):

$$\% \text{ Titan Yellow uptake} = \frac{C_i - C_e}{C_i} \times 100\% \quad (1)$$

$$q_e \text{ (mg/g)} = \frac{(C_i - C_e)V}{M} \quad (2)$$

where;  $C_i$  is initial TY concentration (mg/L),  $C_e$  is concentration of TY (mg/L) at equilibrium,  $V$  is volume of solution (L),  $M$  is weight (g) of LDH.

## RESULTS AND DISCUSSION

### Characterisation

#### FTIR

The FTIR spectrum shows a broad peak at  $3465.19 \text{ cm}^{-1}$  which can be assigned to O-H stretching vibration in the brucite-like layers and the interlamellar water molecules while the broadening of the band is due to the formation of hydrogen bonds. The weak band observed at  $1639.82 \text{ cm}^{-1}$  is assigned to  $\text{H}_2\text{O}$  bending vibration of interlayer water. Sharp peaks at  $1384.11 \text{ cm}^{-1}$  represents symmetric stretching absorption of the carbonate. The peaks below  $1000 \text{ cm}^{-1}$  correspond to  $\text{Mg}^{2+}$ -OH or  $\text{Al}^{3+}$ -OH stretching absorption. Metal-oxygen stretching mode is represented by peaks at  $640.74 \text{ cm}^{-1}$  (Moyo 2009). There was no change in FTIR

**Table 1.** x values for  $\text{MgAl-CO}_3$  and  $\text{MgAl-TY}$

	$\text{MgAl-CO}_3$	$\text{MgAl-TY}$
X	0.33	0.345

**Table 2.**  $2\theta$  and d-spacing values of  $\text{MgAl-CO}_3$  and  $\text{MgAl-TY}$

	Parameter	Peak 1	Peak 2	Peak 3	Average D spacing
$\text{MgAl-CO}_3$	$2\theta$ of the intense peak	$11^\circ$	$23^\circ$	$34.5^\circ$	7.86 Å
	$\theta$ of the intense peak	$5.5^\circ$	$11.5^\circ$	$17.25^\circ$	
	D spacing	8.04 Å	7.73 Å	7.80 Å	
$\text{MgAl-TY}$	$2\theta$ of the intense peak	$11^\circ$	$23^\circ$	$34.5^\circ$	7.86 Å
	$\theta$ of the intense peak	$5.5^\circ$	$11.5^\circ$	$17.25^\circ$	
	D spacing	8.04 Å	7.73 Å	7.80 Å	

spectra before and after adsorption and this is attributed to the absorbance of titan yellow dye which is almost 10 times less than the absorbance of layered double hydroxides (LDH) and layered double hydroxide after adsorption.

#### XRF

Elemental analysis was performed on the XRF. Table 1 shows the atomic ratios of the  $\text{LDH-CO}_3$  and the  $\text{LDH-TY}$  relative to aluminum present. The results for precursor LDH ( $\text{MgAl-CO}_3$ ) shows a value of x of 0.33. The ratio of 2:1 (Mg/Al) obtained from elementary analysis agrees very well with starting ratios of the two metal ions. Analysis of XRF data indicates an x value of 0.345 in the  $\text{LDH-TY}$  obtained from the regeneration method. According to literature, x values for pure  $\text{LDH-CO}_3$  are in the range  $0.22 \leq x \leq 0.33$ . From this point of view the results obtained are in the range for pure hydrotalcite. High x values would have led to the formation of  $\text{Al(OH)}_3$  due to increased number of aluminum octahedra, while low x values would have resulted in the formation of  $\text{Mg(OH)}_2$  sheets due to increased magnesium octahedra (Moyo, 2009).

#### PXRD

The synthesised hydrotalcite d-spacing value of 7.86 Å (Table 2) which is close to literature value of 7.63 Å [24]. In this study, it was established that intercalation of TY did not take place since d-spacing remained at 7.86 Å after the cLDH was in contact with TY. Considering the size of titan yellow there was supposed to be a significant increase in d spacing. It shows that during regeneration carbonate was intercalated as a contaminant instead of the dye anion, this could be avoided by use of an inert atmosphere. Thus the TY was removed from the solution by adsorption on the surface of the particles. PXRD for as synthesized  $\text{Mg-Al-CO}_3$  LDH is shown in Figure 1 and PXRD for regenerated  $\text{Mg-Al-CO}_3$  LDH is shown in Figure 2.

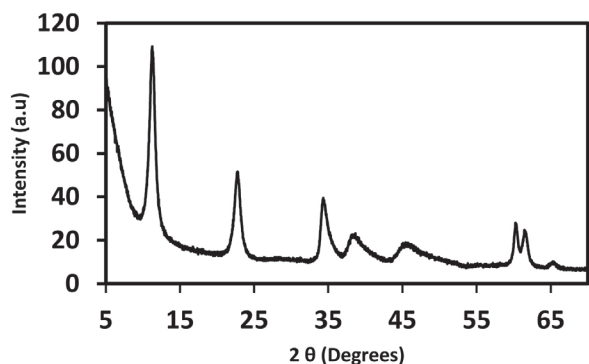


Fig. 1. PXRD for as synthesized Mg-Al-CO<sub>3</sub> LDH

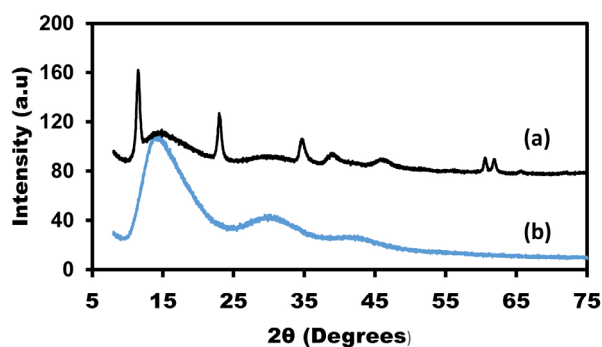


Fig. 2. PXRD for regenerated Mg-Al-CO<sub>3</sub> LDH (a) together with the profile for the glass substrate sample holder (b).

**Effect of initial dye concentration**

The effect of initial concentration was investigated using various dye concentrations (20-100 mg/L) in a fixed time of 3 hr. More increment in contact time did not show significant change in equilibrium concentration; that is, the adsorption process had attained equilibrium as shown in Figure 5. The percentage removal decreased exponentially with the increase in initial TY concentration as a result of reduction of available active sites for adsorption at high concentration, leading to reduced dye removal (Figure 3).

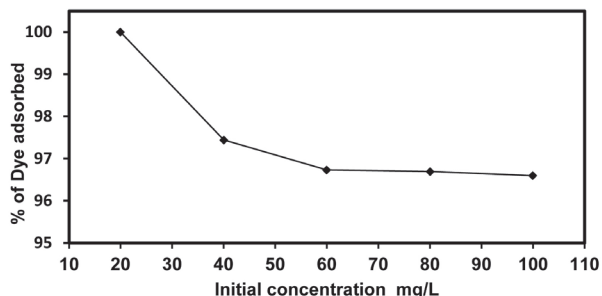


Fig. 3. Effect of initial concentration on adsorption of dye

**Effect of adsorbent dosage**

Effect of adsorbent dosage on dye removal efficiency is represented in Figure 4 and shows an increase in adsorption with increased LDH dosage. For 100 mg/L initial dye concentration, the adsorption efficiency is 96.87 % using 1.0 g LDH compared to 83.63 % removal using 0.2 g. It may be discerned from Figure 4 that adsorption efficiency is approaching maximum at this dosage. Increased dosages had the effect of providing more surfaces and adsorption site; hence increased adsorbent enhances adsorption to a maximum with eventual equilibrium stage.

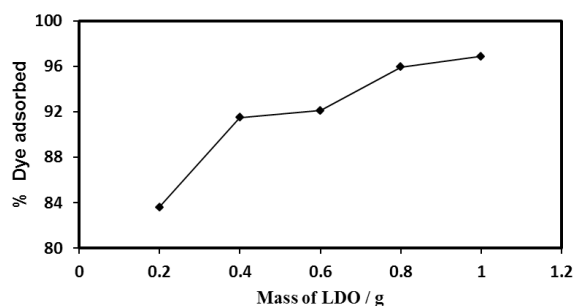


Fig. 4. Effect of cLDH dosage on adsorption of dye

**Effect of contact time**

Effect of contact time between TY and calcined LDH, was studied for 100 mg/L for at least 3 h as shown in Figure 5. Typically, rapid uptake was observed, gradually decreasing with time as equilibrium is attained. The rate of removal was higher initially due to higher available adsorption sites at high concentration at the beginning of contact time. The rate of adsorption is a function of free adsorption sites. As time progressed, the active sites became less accessible, and eventually became saturated. Ideally, in the case of calcined LDH, two types of adsorption sites are available; firstly, the external

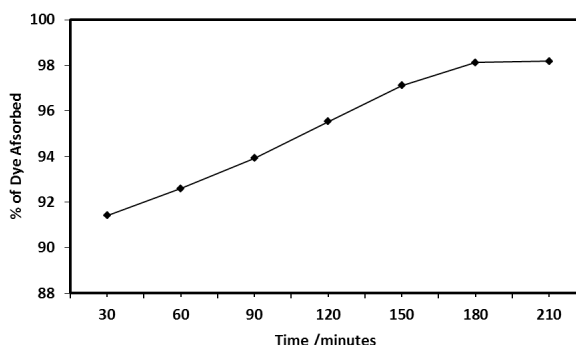


Fig. 5. Effect of contact time on adsorption of dye

surface which leads to surface adsorption, and secondly, within the interlayer region of the host molecule (LDH) (Sumari *et al.*, 2009). Equilibrium adsorption was achieved at about 3 h with maximum removal of 98.38 % for 100 mg/L using 0.8 g sorbent.

### Adsorption Isotherms

Adsorption isotherms of the process were evaluated and experimental data were fitted to four models, Langmuir, Freundlich, Temkin and Dubinin-Radushkevich models which have been widely used to describe metal ion adsorption processes (Abdelhamid *et al.*, 2012; Johnson and Arnold, 1995; Kapoor *et al.*, 1989).

#### Langmuir

The development of the Langmuir isotherm is modelled according to the following premise: each site can hold only a single molecule of the adsorbate without molecular migration, and the energy of adsorption is consistent over the entire surface (Richardson *et al.*, 2002). Maximal adsorption happens when the adsorbate molecule monolayer becomes permeated adjacent to the surface of the adsorbent and along with consistent adsorption energy giving a model in linear (Equation 3):

$$\frac{1}{q_e} = \frac{1}{q_m} + \frac{1}{K_A q_m C} \quad (3)$$

where;  $C$  is concentration at equilibrium of adsorbate (mg/L),  $q_e$  is quantity of metal adsorbed per gram of the adsorbent at equilibrium (mg/g),  $q_m$  is maximum monolayer coverage capacity (mg/g),  $K_A$  is Langmuir isotherm constant (L/mg).

Using a quantity with no dimension, the separation factor  $R_L$  (Equation 4) we can then determine the associated advantage of the process of adsorption under the experimental conditions.

$$R_L = \frac{1}{[1+(1+K_A C_0)]} \quad .. (4)$$

Where  $K_A$  is a constant related to adsorption energy and  $C_0$  is initial concentration.

The Langmuir isotherm assumes that the surface of any adsorbent material contains many active sites to which the adsorbate attaches itself. The model assumes that there is not much interaction between the adsorbed molecules, and no further adsorption will occur once the saturation value is reached. The linear graph obtained by the Langmuir isotherm is shown in Figure 6. The  $R_L$  value is found to be less than 1, indicating that the adsorption process is

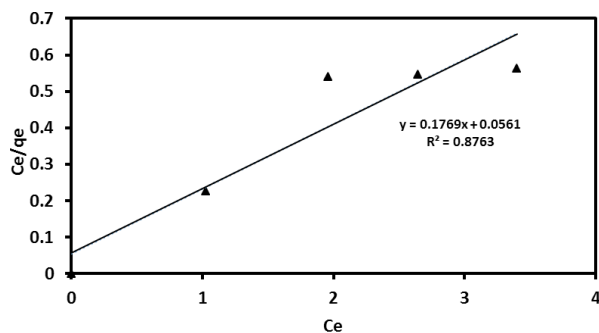


Fig. 6. Langmuir Plot for TY adsorption

favorable. From the plot shown in Figure 6, the following values were estimated:

$$Q_o = 5.6529 \text{ mg/g}, K_A = 3.1534 \text{ and } R^2 = 0.8763.$$

#### Freundlich

The Freundlich isotherm was established on heterogeneous surfaces to simulate multilayer adsorption and the linear form of the model is given in equation 5 (Freundlich 1906):

$$\log q_e = \log K_f + \frac{1}{n} \log C_e \quad .. (5)$$

Where  $q_e$  is amount of metal ions adsorbed in equilibrium (mg/g),  $C_e$  is concentration (ppm) adsorbed at equilibrium,  $K_f$  is Freundlich constant related to capacity of adsorption, and  $n$  is the dimensionless heterogeneity coefficient. The model is based on the following assumption: Adsorption occurs on a heterogeneous adsorption surface, which has unequal available sites and different adsorption energies. Freundlich constants were calculated based on Figure 7 and are presented in Table 3. The calculated value of  $n = 0.9565$  which is below the 1 to 10 range which means Freundlich isotherm was not at play in adsorption. Freundlich's isotherm equation for adsorption of titan yellow is:  $5^{\wedge}_{5R} = 1.7334 C_e = 1.0455$  and  $R^2$  was found to be 0.864.

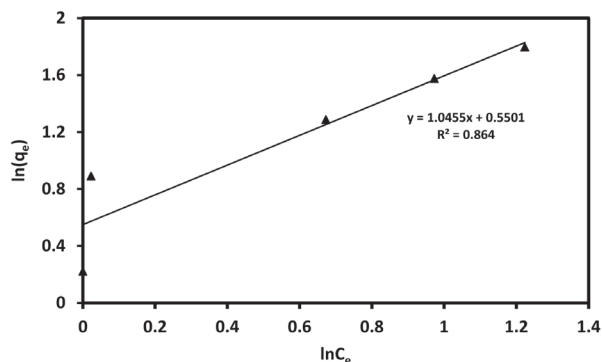


Fig. 7. Freundlich plot for adsorption data

**Temkin**

This isotherm contains a factor that explicitly take into the account adsorbent–adsorbate interactions. By disregarding the low and large figures of concentrations, the model assumes that adsorption heat (temperature function) of molecules in the layer would decrease linearly rather than logarithmically alongside coverage (Temkin and Pyzhev, 1940, Aharoni and Ungarish, 1977). As implied in the equation, its derivation is characterized by a uniform distribution of binding energies (up to some maximum binding energy) was carried out by plotting the quantity sorbed  $q_e$  against  $\ln C_e$  and constants were calculated using the slope and intercept. The model is given by Eq. (6):

$$q_e = B \log A_t + B \log C_e \quad \dots (6)$$

where  $A_t$  is Temkin isotherm binding constant at equilibrium (L/g),  $B_t$  is Temkin isotherm constant, R is gas constant (8.314 J/mol/K), T is Temperature at 298 K, B is Constant related to heat of sorption (J/mol).

From the plot shown in Fig. 8, the following values were estimated:  $\alpha = 1.168$  L/g,  $\beta = 11.036$  J/mol indicating a physical adsorption process and the  $R^2 = 0.9429$ .

**Dubinin-Radushkevich**

Dubinin–Radushkevich isotherm is generally applied to express the adsorption mechanism with a Gaussian energy distribution onto a heterogeneous surface (Gunay *et al.*, 2007; Dabrowski, 2001). The model has often successfully fitted high solute activities and the intermediate range of concentrations data well. The approach has been usually applied to distinguish the physical and chemical adsorption of metal ions. Its mean free energy, E per molecule of adsorbate (for removing a molecule from its location in the sorption space to the infinity) can be computed by the relationship

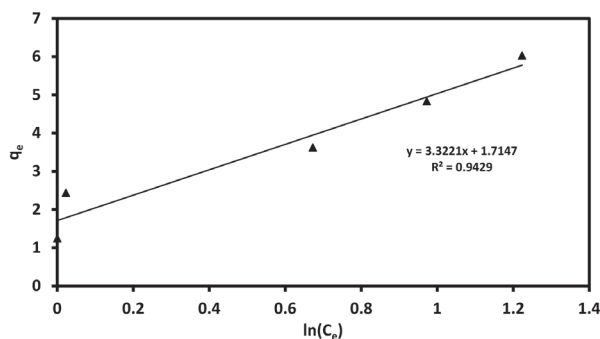


Fig. 8. Temkin Adsorption Isotherm

(Dubinin, 1960; Hobson, 1969). The general equation is expressed as:

$$\text{Log } q_e = \text{Log } q_s - K_{ad} \left[ RT \left( \text{Log } 1 + \frac{1}{C_e} \right) \right]^2 \quad \dots (7)$$

where;  $q_e$  is amount of adsorbate in the adsorbent at equilibrium(mg/g),  $q_s$  is theoretical isotherm saturation capacity (mg/g);  $K_{ad}$  is Dubinin–Radushkevich isotherm constant (mol<sup>2</sup>/Kj<sup>2</sup>) and E is

$$\frac{1}{\sqrt{2BDR}}$$

One of the unique features of the Dubinin–Radushkevich isotherm model lies on the fact that it is temperature-dependent, which when adsorption data at different temperatures are plotted as a function of logarithm of amount adsorbed  $\log q_e$  vs

$\left[ RT \left( \text{Log } 1 + \frac{1}{C_e} \right) \right]^2$  the square of potential energy, all suitable data will lie on the same curve, named as the characteristic curve (Foo and Hameed, 2010).

Dubinin–Radushkevich was applied to express adsorption mechanism with a Gaussian energy distribution on a heterogeneous surface. From the linear plot of DRK model,  $q_m$  was determined to be 2.0087 mg/g, the free energy, E was 0.707 KJ/mol indicating a physisorption adsorption since it is < 50 KJ/mol. The free energy of adsorption increases with temperature. Normally chemisorptions occur at high temperatures. If the free energy is >50 KJ mol<sup>-1</sup>, the nature of adsorption is chemisorptions (Ramachandran *et al.*, 2011). This isotherm has the lowest  $R^2$  value of 0.3691 as shown in Figure 9.

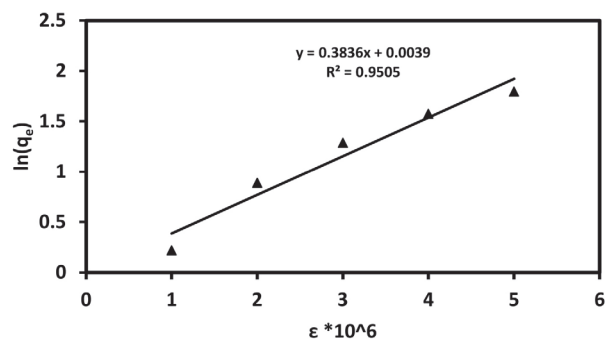


Fig. 9. A plot of the Dubinin-Radushkevich Isotherm

The Dubinin–Radushkevich Isotherm provided the best fit to the experimental data in the adsorption of TY dye onto LDO material, but the calculated adsorption capacity was significantly different from the experimental value. Even though the Langmuir model had a lower correlation

**Table 3.** Summary of adsorption isotherm fitting

Langmuir	
	$q_m = 5.6529$
	$K_A = 3.1534$
	$R_L = (0.031-0.136)$
	$R^2 = 0.8763$
Freundlich	
	$n = 0.9565$
	$K_F = 1.7334$
	$R^2 = 0.864$
Dubinin-Radushkevich	
	$B = 0.3836$
	$q_s = 1.0039$
	$E = 1.30$
	$R^2 = 0.9505$

coefficient, the adsorption capacity is very close to the experimental value (5.7258 mg/g). The parameters are presented in Table 3. The Langmuir separation factor analysis results indicates values between zero and one for the separation factor at all the initial concentrations employed, indicating favorable interactions between the dye and LDO. The analysis also reveal that the reaction was more favourable at higher initial dye concentrations.

### Adsorption Kinetics

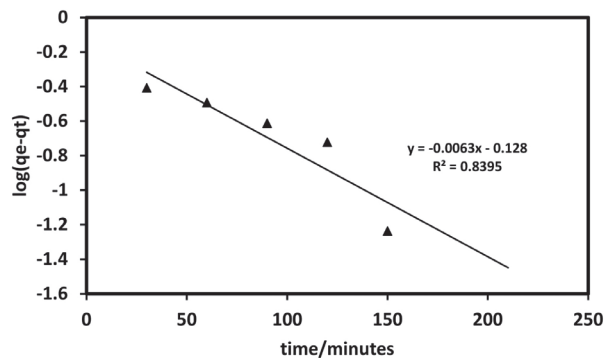
Kinetic modelling of the adsorption process provides a prediction of adsorption rates and allows the determination of suitable rate expressions characteristic of possible reaction mechanisms. The reaction kinetics of the process of adsorption was calculated using the model based approach. Experimental values obtained in the adsorption study was modelled with Elovich, first-order Lagergren and pseudo-second order equations to evaluate the controlling system of the adsorption process (Lagergren and Sven, 1898).

### Pseudo-first order kinetic model

Adsorption goes through several stages, including transporting the adsorbate from the water phase to the surface of the adsorbent, and diffusing the adsorbent to the inside of the adsorbent pores, and then surface reaction with adsorbent molecules. Surface reaction can be modelled using the Lagergren equation which is also referred to as pseudo-first-order model to distinguish a kinetics equation based on the adsorption capacity of a solid from one based on the concentration of a solution. The general equation is expressed as:

$$\log(q_e - q_t) = \log(q_e) - \frac{k_1}{2.303} t \quad \dots (8)$$

Plot according to equation 8 gave  $R^2$  value of 0.8395 shown in Fig 10. Kinetic parameters are shown in Table 4. Results obtained from the experiments did not follow first-order kinetics as shown by the low correlation coefficient value as well as differences in the experimental and calculated adsorption capacity.

**Fig. 10.** Pseudo-First Order

### Pseudo-second order kinetic model

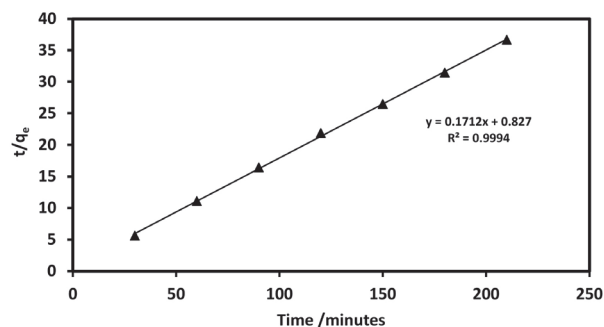
The pseudo-second order rate equation was first applied in heavy metal adsorption by Ho and McKay, 1998 who successfully used it in the competitive removal of heavy metals by Sphagnum moss peat. The modified model has found widespread usage and is expressed as follows:

$$\frac{t}{q_t} = \frac{1}{k_2 q_e^2} + \frac{t}{q_e} \quad \dots (9)$$

The plots according to Equation (9) provided excellent linearity with an  $R^2$  value of 0.9994 as shown in Figure 11. The pseudo second order plot at 100 mg/L initial dye concentration is given in Figure 11 and results of the parameters obtained are given in Table 4.

### Elovich model

The Elovich equation is mainly applicable to chemical adsorption kinetics. This equation is

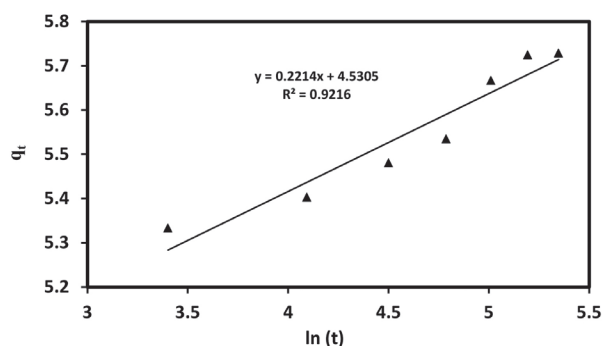
**Fig. 11.** Pseudo Second Order

**Table 4.** Summary of kinetic parameters

Pseudo First Order				
$K_1$ (min <sup>-1</sup> )	$q_e$ cal (mgg <sup>-1</sup> )	$q_e$ exp (mgg <sup>-1</sup> )	$R^2$	
0.0063	0.747	5.7258	0.839	
Pseudo Second Order				
$K_2$ (mgg <sup>-1</sup> min <sup>-1</sup> )	$q_e$ cal (mgg <sup>-1</sup> )	$q_e$ exp (mgg <sup>-1</sup> )	H	$R^2$
0.0242	5.8411	5.7248	1.2092	0.9994
Elovich Model				
$\hat{a}$ (mgg <sup>-1</sup> min <sup>-1</sup> )	$\hat{a}$	$R^2$		
$1.8955 \times 10^8$	4.5167	0.9216		

generally applicable to systems with uneven adsorption surfaces and the more common form is given in equation 10.

$$q_t = \frac{1}{\beta} \ln(\alpha\beta) + \frac{1}{\beta} \ln t \quad (10)$$

**Fig. 12.** Elovich model

Elovich plot for the adsorption of Titan Yellow by cLDH is given in Figure 12 and parameters in Table 4.

The experimental  $q_e$  (exp), calculated  $q_e$  (cal) Figures for pseudo-second order model were close as shown in Table 4. The calculated correlation coefficient is closer to 1 for pseudo-second order kinetics than for pseudo-first order and Elovich kinetic model. The sorption process can be calculated more correctly by the pseudo-second order kinetic model than pseudo-first order and Elovich kinetic models for adsorption of titan yellow onto calcined layered double hydroxide. The rate constant for the reaction was found to be  $2.42 \times 10^{-2} \text{ mg} \cdot \text{g}^{-1} \cdot \text{min}^{-1}$ .

### CONCLUSION

The removal of Titan yellow is dependent on contact time, dosage and initial concentration. Experimental

data gave good fit for the Dubinin-Radushkevich, but Langmuir model provided a better approximation of the adsorption capacity to the experimental value. The results also suggest that adsorption capacity of calcined LDH was found to be 5.6529 mg/g at 25 °C using Langmuir isotherm model that is linearized. Mechanism of adsorption obeys a model that is monolayer and better than an isotherm model that is heterogenous. Favourability of the process of adsorption is reflected by a Langmuir dimensionless separation factor  $R_L$  (0.031-0.136). From the  $R_L$  values it can be concluded that since it is between 0 and 1 the Langmuir Isotherm is favourable. The kinetics of the adsorption followed pseudo second order model with the rate constant .

### REFERENCES

- Abdelhamid, B., Ourari, A. and Ouali, M.S. 2012. Copper (II) Ions Removal from Aqueous Solution Using Bentonite Treated with Ammonium Chloride. *Am. J. Phys. Chem.* 1 : 1-10.
- Aharoni, C. and Ungarish, M. 1977. Kinetics of activated chemisorption. Part 2. Theoretical models. *J. Chem. Soc., Faraday Trans.* 1 (73) : 456-464.
- Al-Degs, Y., Khraisheh, M.A.M., Allen, S.J. and Ahmad, M.N.A. 2001. Sorption behavior of cationic and anionic dyes from aqueous solution on different types of activated carbons. *Sep. Sci. Technol.* 36 : 91-102.
- Banerjee, S. and Chattopadhyaya, M.C. 2017. Adsorption characteristics for the removal of a toxic dye, tartrazine from aqueous solutions by a low cost agricultural by-product. *Arabian Journal of Chemistry.* 10 (2) : 1629-1638.
- Dabrowski, A. 2001. Adsorption-from theory to practise. *Advances in Colloid and Interface Science.* 93 : 135-224.
- Dubinin, M.M. 1960. The potential theory of adsorption of gases and vapours for adsorbents with energetically non-uniform surface. *Chemistry*



- Reviews*. 60 (96) : 235-266.
- Fan, G., Li, F., Evans, D.G. and Duan, X. 2014. Catalytic applications of layered double hydroxides: recent advances and perspectives. *Chem. Soc. Rev.* 43 : 7040-7066.
- Foo, K.Y. and Hameed, B.H. 2010. Insights into the modelling of adsorption isotherm systems. *Chemical Engineering Journal*. 15(6) : 2-10.
- Freundlich, H.M.F. 1906. Über Die Adsorption in Losungen. *Z. Phys. Chem.* 57 : 385-470.
- Gómez, V., Larrechi, M.S. and Callao, M.P. 2007. Kinetic and adsorption study of acid dye removal using activated carbon. *Chemosphere*. 69 : 1151-1158.
- Greluk, M. and Hubicki, Z. 2011. Efficient removal of Acid Orange 7 dye from water using the strongly basic anion exchange resin Amberlite IRA-95. *Desalination*. 278 (1-3) : 219-226.
- Gunay, A., Arslankaya, E. and Tosun, I. 2007. Lead removal from aqueous solution by natural and pretreated clinoptilolite: adsorption equilibrium and kinetics. *Journal of Hazardous Materials*. 6 (7) : 362-371.
- Gupta, V.K., Kumar, R., Nayak, A., Saleh, T.A. and Barakat, M.A. 2013. Adsorptive removal of dyes from aqueous solution onto carbon nanotubes: a review. *Adv Colloid Interface Sci.* 193-194, 2434.
- Hobson, J.P. 1969. Physical adsorption isotherms extending from ultra-high vacuum to vapour pressure. *J. Phys. Chem.* 7 (3) : 2720-2727.
- Johnson, R.D. and Arnold, F.H. 1995. The Temkin Isotherm Describes Heterogeneous Protein Adsorption. *Biochim. Biophys. Acta*. 1247: 293-297.
- Kapoor, A., Ritter, J.A. and Yang, R.T. 1989. On the Dubinin-Radushkevich equation for adsorption in microporous solids in the Henry's law region. *Langmuir*. 5 (4) : 1118-1121.
- Kurniawan, T.A., Chan, G.Y.S., Lo, W.H. and Babel, S. 2006. Physico-chemical treatment techniques for wastewater laden with heavy metals. *Chemical Engineering Journal*. 118(1-2): 83-98.
- Kyzas, G.Z. and Matis, K.A. 2018. Review-Flotation in Water and Wastewater Treatment. *Processes*. 6: 116-132.
- Lagergren, S. and Sven, K. 1898. About the theory of so-called adsorption of soluble substances. *Sven. Vetensk. Handl.* 24 : 1-39.
- Marsch, H. and Reinoso, F.R. 2006. Activated Carbon, Elsevier: Amsterdam.
- Mehrijouei, M., Müller, S. and Möller, D. 2015. A review on photocatalytic ozonation used for the treatment of water and wastewater. *Chemical Engineering Journal*. 263 (1) : 209-219.
- Mir, S.H., Nagahara, L.A., Thundat, T., Mokarian-Tabari, P., Furukawa, H. and Khosla, A. 2018. Review—Organic-Inorganic Hybrid Functional Materials: *An Integrated Platform for Applied Technologies Journal of The Electrochemical Society*. 165 (8) B3137-B3156.
- Mishra, G., Dash, B. and Pandey, S. 2018. Layered double hydroxides: A brief review from fundamentals to application as evolving biomaterials. *Applied Clay Science*. 153 : 172-186.
- Moyo, L. 2009. A critical assessment of the methods for intercalating anionic surfactants in layered double hydroxides. Msc. Dissertation, University of Pretoria, South Africa, 1-75.
- Pereira, M.F.R., Soares, S.F., Orfao, J.J.M. and Figueiredo, J.L. 2003. Adsorption of dyes on activated carbons: influence of surface chemical groups. *Carbon*. 41 : 811-821.
- Pérez, G., Fernández-Alba, A.R., Urriaga, A.M. and Ortiz, I. 2010. Electro-oxidation of reverse osmosis concentrates generated in tertiary water treatment. *Water Research*. 44 (9) : 2763-2772.
- Richardson, J.F., Harker, J.H. and Backhurst, J.R. (eds.) 2002. *Coulson and Richardson's Chemical Engineering, Particle Technology and Separation Processes*. 2, 5th ed., Butterworth-Heinemann, Oxford, UK.
- Sarfraz, M. and Shakir, I. 2017. Review-Recent advances in layered double hydroxides as electrode materials for high-performance electrochemical energy storage devices. *Journal of Energy Storage*. 13: 103-122.
- Sen, T.K. and Dawood, S. 2014. Review on Dye Removal from Its Aqueous Solution into Alternative Cost Effective and Non-Conventional Adsorbents. *J Chem Proc Engg.* 1 : 1-11.
- Shen, Q., Zhua, J., Cheng, L., Zhang, J., Zhang, Z. and Xu, X. 2011. Enhanced algae removal by drinking water treatment of chlorination coupled with coagulation. *Desalination*. 271(1-3) : 236-240.
- Sumari, S.M., Yasin, Y. and Hamzah, Z. 2009. Adsorption of anionic amido black dye by layered double hydroxide, ZnAlCO<sub>3</sub>-LDH. *The Malaysian Journal of Analytical Sciences*. 13 (1) : 120-128.
- Temkin, M. and Pyzhev, V. 1940. Kinetics of Ammonia Synthesis on Promoted Iron Catalysts. *Acta Physicochimica URSS*. 12 : 217-222.
- Xu, P., Capito, M. and Cath, T.Y. 2013. Selective removal of arsenic and monovalent ions from brackish water reverse osmosis concentrate. *Journal of Hazardous Materials*. 260 : 885-891.
- Xu, T. 2005. Review-Ion exchange membranes: State of their development and perspective. *Journal of Membrane Science*. 263 (1-2) : 1-29.
- Zümreoglu-Karan, B. and Ay, A.N. 2012. Review-Layered double hydroxides - multifunctional nanomaterials. *Chemical Papers*. 66 (1) : 1-10.
- Zaharia, C. and Suteu, D. 2012. Textile Organic Dyes - Characteristics, Polluting Effects and Separation/Elimination Procedures from Industrial Effluents - A Critical Overview, Organic Pollutants Ten Years After the Stockholm Convention - Environmental and Analytical Update, Dr. Tomasz Puzyn (Ed.), ISBN: 978-953-307-917-2, InTech.
-